

COMMISSIONING OF A NEW DOSE RATE MONITORING SYSTEM AT THE S-DALINAC*

J. Birkhan[†], M. Arnold, U. Bonnes, J. Conrad, M. Hess, L. Marc, N. Pietralla, L. Stobbe, P. v. Neumann-Cosel, Institute for Nuclear Physics, Darmstadt, Germany

Abstract

Recently a new radiation protection interlock system has been established at the Darmstadt superconducting linear electron accelerator S-DALINAC. It prevents the staff from entering radiation protection areas during operation and allows a systematic scanning of these areas for workers before running the accelerator. As an extension of the new interlock, a new dose rate monitoring system has been developed using PIN-diode arrays and self-made ion chambers. These detectors will be used to perform online dose rate measurements in order to switch automatically the status of illuminated radiation protection panels, which show the current level of protection area.

INTRODUCTION

Operating a charged-particle accelerator results in the production of ionizing radiation and the irradiation of its environment. The S-DALINAC is a superconducting recirculating electron accelerator that is operated in an energy range of 10 MeV (@ 60 μ A) to 130 MeV (@ 20 μ A). When the beam transport has been optimized the primary ionizing radiation is dominated by synchrotron radiation and, for example in the case of nuclear resonance fluorescence experiments, by bremsstrahlung. At beam energies larger than the neutron separation threshold one has to expect neutron fluxes as well. These neutron fluxes, but also the bremsstrahlung, produce radioactive isotopes in the environment of the accelerator, for example Co-60 in steel or Na-22 in aluminum [1, 2]. The dose rates during operation and afterwards due to activation products can reach levels that the national radiation protection regulation has to be applied [3, 4]. Therefore, the accelerator and experimental hall as well as closely related technical rooms are declared as radiation areas to protect the workers against unreasonable exposure situations. While nuclear structure experiments are performed at the S-DALINAC the accelerator and experimental halls are restricted areas (potential local dose rate: $\dot{H} > 3$ mSv/h). Then, the closely related technical rooms are controlled areas (potential effective dose per 2000 h/a: $E > 6$ mSv). When no beam is prepared and no high frequency signal is fed to the cavities these halls and technical rooms are supervised areas (potential effective dose per 2000 h/a: $E > 1$ mSv). The current status of a radiation area is shown by an illuminated three-level panel in front of the doorways of that area, see Fig. 1. When beam and high frequency signals have been switched off the licensee has to validate that the dose rates do not exceed the regulatory

limit of a supervised area. At the S-DALINAC, this has been done so far by manual measurements only. To prevent the radiation protection officer from potential exposure situation and to save time an online measurement system has been designed which will be permanently installed inside the radiation areas. It will also allow to perform long term monitoring while operating the S-DALINAC. Furthermore, such a detector setup can be used to improve the beam diagnostics as well.

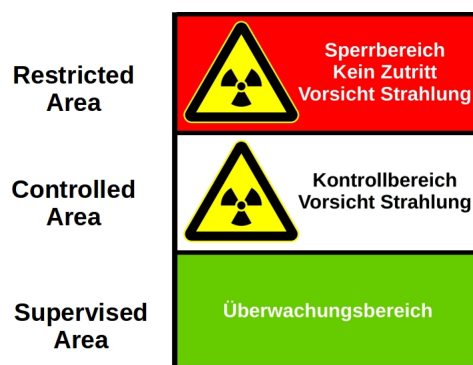


Figure 1: Radiation protection panel distinguishing the different radiation protection levels.

ARCHITECTURE

The new dose rate monitoring system consists of radiation detectors which are read out by micro controller boards (μ C). Two boards have been used: the Nucleo-F767ZI [5] and the Arduino-UNO with ethernet shield [6]. If the measured signal exceeds a certain threshold the μ C switches a relay which is connected to the personal interlock system (PIS) [7], see Fig. 2. The PIS is also responsible for controlling the illuminated radiation panels and to switch between the three levels. The new detector systems allow to measure the local dose rates before the level of radiation area is set from restricted or controlled to supervised. Furthermore, the online measured data can be accessed via the μ C ethernet interface. The μ C are device servers which can easily be integrated into the EPICS-based control system using the EPICS stream device support [8, 9].

TESTED DETECTOR TYPES AND ELECTRONICS

Dosimetry has a long standing history of using geiger-tube counters and ion chambers [10–12], especially for examining environmental radiation-exposure situations [13]. Today, small semiconductor detectors are also capable of measuring

* Work supported by RTG2128

[†] jbirkhan@ikp.tu-darmstadt.de

Content from this work may be used under the terms of the CC BY 3.0 licence (© 2017). Any distribution of this work must maintain attribution to the author(s), title of the work, publisher, and DOI.

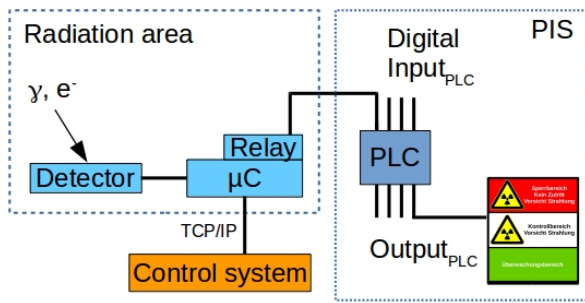


Figure 2: Layout of the new dose rate monitoring system at the S-DALINAC, (PIS = Personal Interlock System, PLC = Programmable Logic Controller).

low dose rates due to sufficient sensitive and low-noise read-out electronics. Semiconductor detectors are already in use as beam-loss monitors at the S-DALINAC [14]. Low-cost geiger tubes suffer from the disintegration of the organic quenching gas as well as from a too large dead time, if they are used in high photon- or particle-flux environments. Semiconductor detectors, like the beam-loss monitors from above, suffer from low photon efficiencies. They need to measure for a longer period of time to provide a count rate with a certain precision. If dose rates need to be measured only, an air-filled ion chamber overcomes these problems. If the ion chamber is read out with a suitable operational amplifier as part of charge-sensitive amplifier circuit [15], then the measurand is a continuous voltage as function of the electron-ion pairs produced by the incident radiation. Furthermore, the physics of ion chambers is well understood and they are proven to run stable [13,16]. Inspired by projects that favour homemade ion chambers [12, 17] and that use PIN-diode array detectors [18], the decision was made to build ion chambers and use RD3024 detectors from TEVISO [19].

Homemade Ion Chamber

For simplicity a first prototype was built from cylindrical tin cans. The ion-chamber setup consists of an inner zinc-coated can, the ion chamber (height = 75 mm, diameter = 80 mm), and an outer can (height = 115 mm, diameter = 100 mm). The outer can covers the inner ion chamber and shields it against high frequency signals. The bottom of the inner can is covered by an aluminum foil, the bottom of the outer can by a steel grid (mesh size = 1 mm x 1 mm). The inner can is mounted and isolated against the outer can by using teflon and polystyrene spacer, see Fig. 3 on the left. The anode wire of the ion chamber is made of copper (length = 65 mm, diameter 0.5 mm). It is mounted on the top of the outer can by the inner pin of a BNC connector. The inner pin of a second BNC connector pulls the inner can down to ground. The chamber is driven by a voltage of 30 V (10 x 3 V button cells). The charge-sensitive amplifier circuit is shown in detail in Fig. 4. The maximum voltage, that can be measured, is limited by the support voltage of the operational amplifier. The amplifier setup was mounted on the top of the shielding can. An additional shielding can covers the amplifier setup

and is soldered to the first one. A small hole is drilled into the top shielding in order to let the signal cable come out.



Figure 3: Ion chamber made from cylindrical cans. The outer can provides a shielding against high frequency signals, for further details see text.

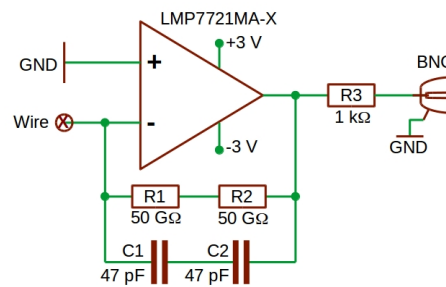


Figure 4: Charge-sensitive amplifier for the read-out of the homemade ion chamber.

Semiconductor Detector

The semiconductor detector RD3024 is based on an array of PIN diodes. The integrated pulse discriminator provides TTL signals which can be counted by a counter input of one of the previous described μC boards. The sensor is capable of detecting electrons and gamma radiation. It is designed for dose rates between 0.1 $\mu\text{Sv/h}$ and 100 mSv/h , assuming an energy range of 50 keV to 1.3 MeV. This fits to the photon energies of most of the activated radioisotopes. The detector needs a small RC-filter circuit that allows to increase the resistivity against high frequency signals. Measurements very close to the cryostats of the S-DALINAC have shown that an additional shielding improves the resistivity further. Therefore, the whole setup was mounted in an aluminum box with a few small holes for venting.

MEASUREMENTS

Test measurements have been performed with both detector types:

1. All detectors were placed very closely together at a certain point in the accelerator hall. It was expected to have a nearly homogeneous radiation flux at this point. Additionally a calibrated dose meter was measuring the dose rate at the same point. In order to enlarge the

dose rates the beam current was increased stepwise at a beam energy of 2.5 MeV. The detectors were exposed against dose rates from 10 $\mu\text{Sv/h}$ to 64 $\mu\text{Sv/h}$.

2. A calibration source (Co-60) was placed in front of the ion chamber. The distance between each detector and source was modified in order to produce different dose rates. The dose rates were calculated from the known activity of the source and the distance. The ion chamber was exposed against dose rates from 0.3 $\mu\text{Sv/h}$ to 1.4 $\mu\text{Sv/h}$. A similar calibration has been done for the RD3024 but using Am-241 and Cs-137 as well at three different distances. The dose rates ranged from 0.5 $\mu\text{Sv/h}$ to 2.0 $\mu\text{Sv/h}$.

Homemade Ion Chamber

The calibration measurement of the ion chamber according to item 1 shows a clear structure related to the stepwise increase of the radiation flux, see Fig. 5. The largest uncertainty of the voltages at each plateau is smaller than 4 %, including beam-current instabilities. Assuming a linear response function the largest detectable dose rate is about 310 $\mu\text{Sv/h}$ (≈ 3 V).

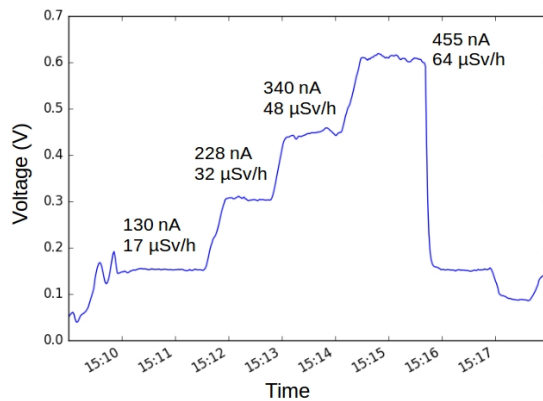


Figure 5: Calibration measurement of the homemade ion chamber. Beam current and dose rate are shown for every plateau. The beam energy was 2.5 MeV.

The calibration measurement of the ion chamber according to item 2 is shown in Fig. 6. The asymmetric uncertainties immediately attract ones attention. They result from nuisance signals which are well separated from the very stable base-line signal caused by the calibration source, see Fig. 7. These nuisance signals are always positive. Therefore, the frequency distribution of the measured voltages is asymmetric. If the reason for them can be found, for example cosmics, they can be removed from the data sets. Under this assumption all pairs of measured voltages would be significantly different from each other and from the environmental radiation background. Then, the detection limit would amount 30 nSv/h which fits the radiation background in many offices of the institute.

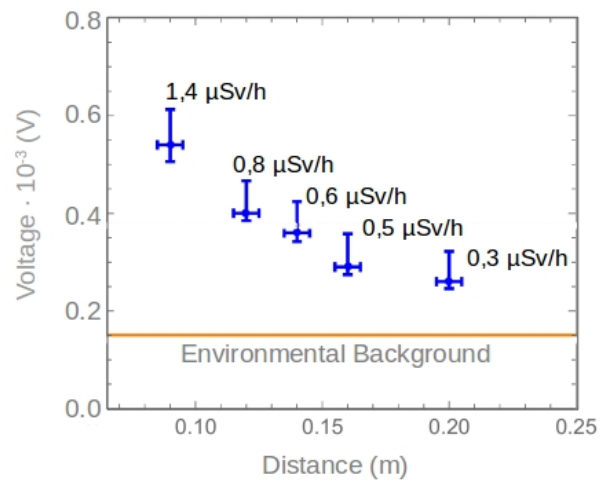


Figure 6: Calibration measurement of a RD3024 detector. A Co-60 source was placed in front of the detector at different distances. The dose rates were calculated from the distances and the activity of the source.

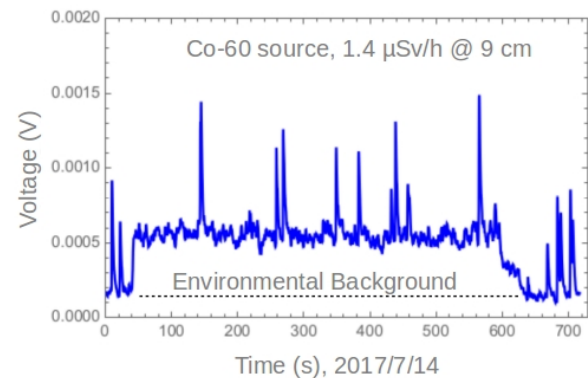


Figure 7: On the top of the signal-base line some nuisance signals occur. The amplitudes of these signals form a relatively narrow gaussian distribution. The repetition rate of the nuisance signals is independent of the incident radiation flux.

Semiconductor Detector

The calibration measurement of the RD3024 according to item 1 is shown in Fig. 8. If the number of counting events is recorded per second it becomes obvious that large fluctuations occur which make it impossible to identify the stepwise increase of the beam current. A larger amount of events needs to be accumulated before the dose rate is calculated. This can be done by extending the measurement time per dose rate value. It could be shown that this problem will be significantly smaller at higher radiation fluxes. The calibration measurement of the RD3024 according to item 2 was used to evaluate the parameters of a linear response function. After that a radioactive source was measured. The source was known to expose the detector against a dose rate of (1.2 ± 0.3) $\mu\text{Sv/h}$. The measurement result was (1.2 ± 0.1) $\mu\text{Sv/h}$.

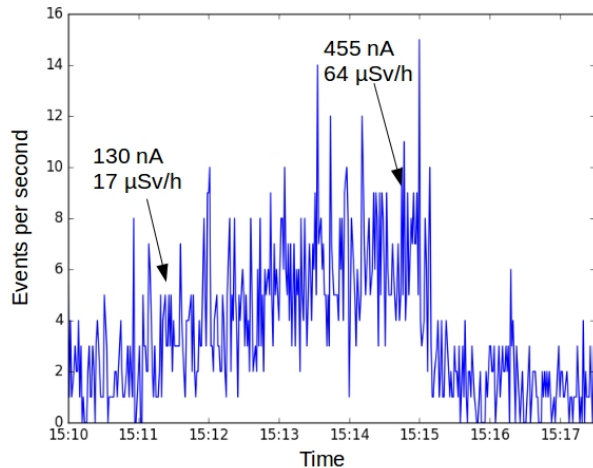


Figure 8: Calibration measurement of a RD3024 detector. Beam current and dose rate are shown for the first and last plateau. The beam energy was 2.5 MeV.

CONCLUSION AND SUMMARY

The measurements have shown that the handmade ion chamber is capable of measuring background-radiation levels as well as dose rates up to 64 $\mu\text{Sv/h}$. Assuming a linear response function it is expected that the chamber will be able to operate up to 310 $\mu\text{Sv/h}$. If the problem of the nuisance signals can be solved the ion chamber is the favoured detector for the dose rate monitoring system. The ion-chamber setup is simple and the continuous output voltage can easily be measured with a sufficient high precision. This setup can operate as beam-loss monitor if an amplifier with a larger operating range is used. Additionally the efficiency of the chamber can be reduced by building a smaller one. The RD3024 detectors can be used as well for the monitoring system as far as it is acceptable to wait about 3 min to 10 min for a reliable measurement result. They could also serve as beam-loss monitors in a S-DALINAC like environment. Currently two RD3024 are permanently in operation to measure dose rates at different locations inside the accelerator hall. These measurements allow to create a dose rate map. The map will be used to find out the locations where to mount detectors permanently for switching the illumination of the radiation panels.

REFERENCES

[1] L. Stobbe, "Simulation von Strahlungsflüssen am S-DALINAC mit FLUKA und Inbetriebnahme von PIN-Diodendetektoren und einer Ionisationskammer für Dosisleistungsmessungen", B.Sc. thesis unpublished, Institute for Nuclear Physics, TU Darmstadt, Germany, 2017.

[2] L. Marc, "Strahlenschutzrelevante Charakterisierung der Beschleunigerhalle des S-DALINACS", B.Sc. thesis unpublished, Institute for Nuclear Physics, TU Darmstadt, Germany, 2017.

[3] ICRP (International Commission on Radiological Protection), "2007 Recommendations of the International Commission on Radiological Protection (Users Edition)", ICRP Publication 103, *Ann. ICRP* 37 (2–4), 2007.

[4] H.M. Veith, "Strahlenschutzverordnung: Textausgabe mit einer erläuternden Einführung", Bundesanzeiger Verlag, 2016.

[5] ST, <http://www.st.com>

[6] Arduino, <http://www.arduino.cc>

[7] M. Arnold *et al.*, "The new PLC based Radiation Safety Interlock System at S-DALINAC", in *Proc. IPAC'14*, Dresden, Germany, 2014, pp. 1802–1804, doi:10.18429/JACoW-IPAC2014-TUPRI098

[8] C. Burandt *et al.*, "The EPICS-based accelerator control system of the S-DALINAC", in *Proc. ICALEPCS'13*, San Francisco, CA, USA, 2013, pp. 332–335.

[9] EPICS, <http://www.aps.anl.gov/epics>

[10] W. K. Sinclair, "Comparison of Geiger-Counter and Ion-Chamber Methods of Measuring Gamma Radiation", *Nucleonics*, vol. 7, no. 6, pp. 21–26, Dec. 1950.

[11] A. Sewkor, "Measurement of Very High Dose Rate of Ionization Radiation by Ionometric Method", *Biophysik*, vol. 3, pp. 8–10, Nov. 1965.

[12] J. O. Silva *et al.*, "Characterization of a new ionization chamber in radiotherapy beams: Angular dependence and variation of response with distance", *Applied Radiation and Isotopes*, vol. 70, no. 10, p. 2534–2538, Oct. 2012.

[13] H. Krieger, "Strahlungsmessung und Dosimetrie", Springer Fachmedien Wiesbaden, Springer Spektrum, 2013.

[14] R. Stegmann *et al.*, "Installation and Test of a Beam Loss Monitor System for the S-DALINAC", *Proc. IPAC'12*, New Orleans, LA, USA, 2012, pp. 804–806.

[15] J. F. Keithley *et al.*, "Low Level Measurements", Kethley Instruments, Inc., Cleveland, Ohio, USA, 1984.

[16] R. Ravichandran *et al.*, "Estimation of absorbed dose in clinical radiotherapy linear accelerator beams: Effect of ion chamber calibration and long-term stability", *Journal of Medical Physics*, vol. 38, no 4, pp. 205–209, Oct. 2013.

[17] TECHLIB, <http://www.techlib.com>

[18] Theremino, <http://www.theremino.com>

[19] TEVISO, <http://www.teviso.com>

Content from this work may be used under the terms of the CC BY 3.0 licence (© 2017). Any distribution of this work must maintain attribution to the author(s), title of the work, publisher, and DOI.